ARTICLE

Molecular Dendritic Transporter Nanoparticle Vectors Provide Efficient Intracellular Delivery of Peptides

Sharon K. Hamilton and Eva Harth*

Department of Chemistry, Vanderbilt Institute of Nanoscale Science and Engineering, Vanderbilt Institute of Chemical Biology, Vanderbilt University, 7619 Stevenson Center, Nashville, Tennessee 37235

ABSTRACT We present the synthesis of a modular delivery system that is composed of two main macromolecular building blocks, dendritic molecular transporter molecules and a polymeric scaffold in a size dimension of 5—10 nm. The conjugated dendritic molecular transporter units proved to be critical for the delivery of the polymer nanoparticle into 3T3 cells and illustrates the dendritic molecular transporter promoted intracellular uptake of polymer particles derived from intramolecular chain collapse processes. In a sequence of modification steps, pyridinyldithio linker was introduced to undergo thiol—disulfide exchange reactions with peptide sequences containing cysteine amino acid units to furnish peptide—nanoparticle conjugates with cleavable disulfide linkers. The intracellular uptake of the nanoparticle conjugates and the delivery of the peptidic cargo were studied *via* dual labeling of the nanoparticle with Alexa Fluor 568 dye and fluorescein (FITC) markers on the peptide in mammalian cell lines such as NIH 3T3 cells *via* confocal microscopy. In this work, we have demonstrated the assembly of a novel nanoscopic delivery system in which the conjugated dendritic molecular transporter molecules facilitated the rapid cellular uptake of a nanoparticle—peptide conjugate with up to 25 copies of peptidic cargo to establish new venues for the implementation of protein and oligonucleotide drugs.

KEYWORDS: dendritic molecular transporter · peptide delivery · nanomedicine · nanoparticle · macromolecular building blocks · transport across biological barrier · nanobiotechnology

The discrepancy between the progress in the development of highly potent drugs and the ability to selectively administer these moieties to reach their targets and intracellular locations has given delivery strategies facilitating transport across biological barriers one of the highest prospective for future breakthroughs in therapy. So far, limitations in efficacy apply not only to highly toxic small molecules; it is especially evident with macromolecular medicines like peptides, oligonucleotides, and antibodies.[1] Only a fraction of small and macromolecular agents reach their biological targets *in vivo*, so intracellular delivery of various drugs can sharply increase the efficiency of various treatment protocols.[2] Because the plasma membrane is very selective and only molecules with the appropriate range of molecular size, polarity, and charge are able to cross the membrane, the therapeutic efficacy can be increased if approaches for direct cytoplasmic delivery are developed, which is especially important for many anticancer reagents, gene, and protein drugs.[3]

Strategies for an increased intracellular uptake of therapeutics have included the utilization of membrane-permeable peptides such as the Tat protein and nonaarginines (R9).[4,5] For example, cell- penetrating peptides have been attached to liposomal carriers and micelles, and an enhanced uptake of the carriers has been evaluated.[2,6] Macromolecular synthesis approaches to design peptide mimics, end functionalized with guanidine groups, are also attractive and gaining importance as building blocks to circumvent polypeptide synthesis and to guarantee a higher metabolic stability.[7−11] On the basis of our studies, we found that polyamide-based dendrimer backbones, known as Newkome dendrimers, in which the peripheral guanidine groups are connected and differentiated with alkyl chains of varied length to the dendritic backbone, showed rapid uptake and were observed in contrary subcellular locations.[10] The evaluation of the transport abilities of not only small molecules such as fluorophore dyes but also macromolecular bioactive materials was demonstrated with the uptake of monoclonal IgG antibodies (5 × 15 nm) into infected cells.[12] To allow the bioactive material to execute function in the native state, a disulfide unit was introduced between the antibody and the dendritic architecture to provide cleavage under the reductive conditions in cells. The inhibition of viral production proved the non-altered biological activity of the antibody along with a higher efficacy of the IgG through the intracellular delivery.[12] It was our goal to extend this concept to the delivery of macromolecules of lower molecular weight

*Address correspondence to eva.harth@vanderbilt.edu.

Received for review October 10, 2008 and accepted January 06, 2009.

Published online February 5, 2009.
10.1021/nn800679z CCC: $40.75

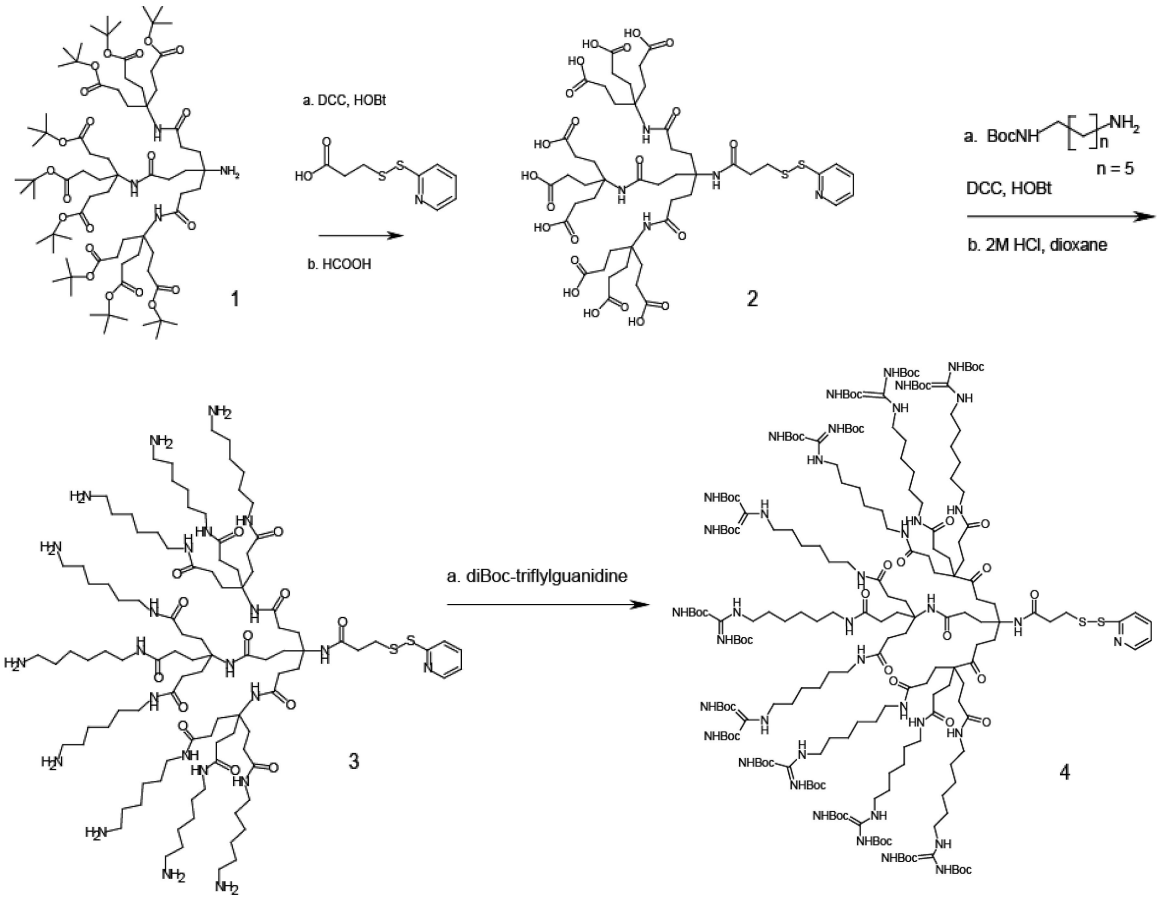

Scheme 1. Synthesis of molecular transporter 4 with conjugated disulfide linker at the focal point.

that also require rapid uptake and tools for internalization.

Peptides have found extensive utilization as extracellular targeting units, but the increasing interest in peptide therapeutics has led to several strategies for their delivery. One of the methods included the alteration of peptide drugs *via* introduction of chemical braces in the polyamide backbone, which led to permanent conformational changes and resulted in increased bioavailability.[13,14] These stapled α-helices or strapped down helices show an enhanced stability and cellular uptake, which has intensified the interest to apply peptide therapeutics in protein−protein interactions inside the cell. Rather than altering peptide structures or oligonucleotide therapeutics to enhance uptake with so far unknown biological consequences, we sought to develop carrier systems that will enable the rapid uptake of multiple copies of peptides that maintains fully the biological structure of the peptide once transported across the cellular membrane. Here, we planned to integrate the dendritic molecular transporter, but in contrast to the discussed antibody−dendritic molecular transporter conjugate,[12] the peptides were not directly attached to the transporter molecule but rather to a nanoparticle scaffold over cleavable disulfide linkers, whereas the molecular transporter units are directly conjugated to the nanoparticle backbone. With this, a higher drug load of macromolecular therapeutics can be achieved than a direct conjugation to the dendritic molecular transporter molecule. As a nanoparticle scaffold, we chose to modify 3-D cross-linked linear hydrophilic polymers resembling protein structures in size dimensions of 5−10 nm.[15,16] These well-defined structures of less than 25 nm allow the integration of multiple functional groups and facilitate sequential modifications to conjugate molecular transporter molecules and peptidic therapeutics. In contrast to traditional delivery systems such as liposomes,[17,18] the carrier is more than a magnitude smaller, with the intent to avoid reported accumulation of larger structures above 30 nm in the liver and spleen or to show immunogenetic reactions as caused from delivery with viral capsules.[19,20] Furthermore, the concentration of positive charge that can cause unwanted interactions with serum *in vivo* could be addressed by the sequential attachment strategy for an increased flexibility in the amount of positively charged molecular transporter units conjugated to the selected nanovector. Additionally, rather than encapsulating the linear peptides, we sought a covalent attachment that would release the valuable peptide load in the cell for a more controlled delivery of the therapeutics. This work documents the design and synthesis of nanocarriers that utilize hydrolytically stable dendritic molecular transporters to-

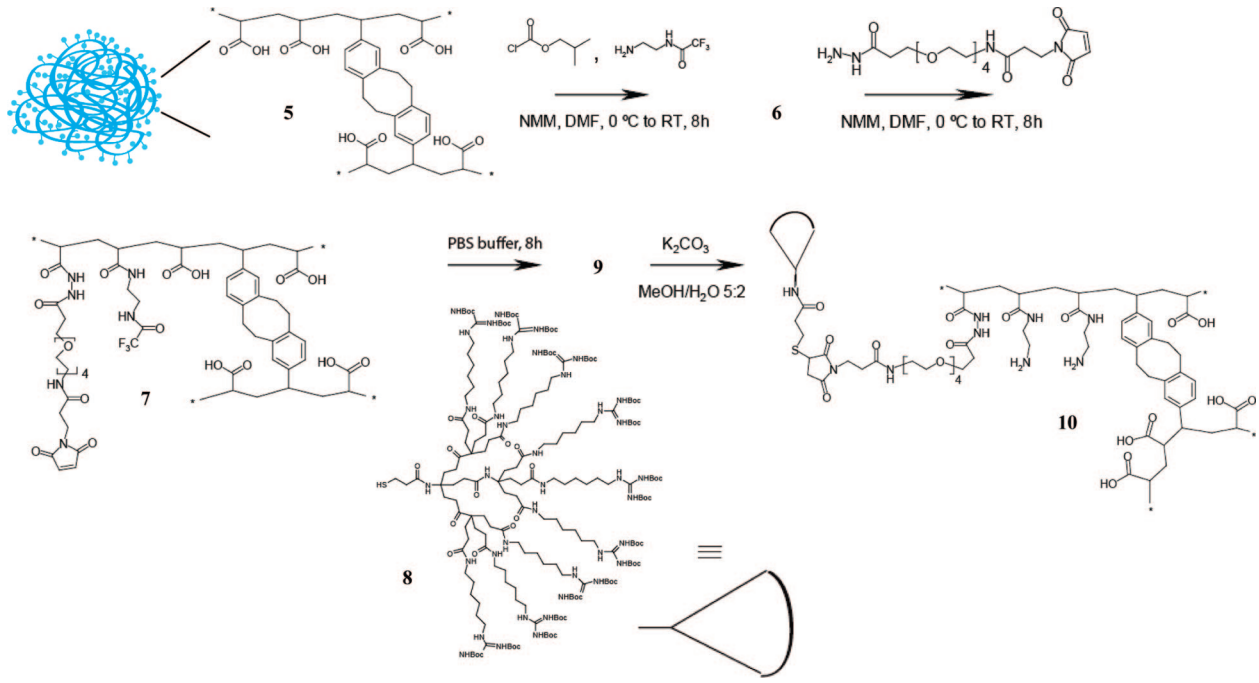

Scheme 2. Synthesis of nanoparticle conjugates.

gether with the smallest known polymeric nanoparticle to form a compact delivery system for the rapid delivery of therapeutics. The sequential modification strategy allows the consecutive adjustment of cell-penetrating units and disulfide linkers that determine the number of peptide units attached. Moreover, the influence of the dendritic cell-penetrating unit to internalize the nanoparticle conjugate is investigated and provides an initial proof of concept to further expand the application to the delivery of oligonucleotides such as siRNA.

RESULTS AND DISCUSSION

We began the synthesis of the macromolecular drug delivery system with the design of one of the critical macromolecular building blocks. As previously reported, we have synthesized dendritic molecular transporter molecules that show contrary subcellular localization profiles governed by an alkyl linker differentiation between the dendritic scaffold and the peripheral guanidine end groups.[10] We sought to utilize these transporter molecules for the delivery of biologically relevant cargo, and we selected a number of chemoselective linkers that would serve as conjugation tools to therapeutics and delivery scaffolds. We intended to provide a cleavable linker that releases the cargo under reductive conditions of the cell cytoplasm or would undergo a thiolene-type reaction and react with activated double bonds such as maleimides. A suitable pyridinyldithio moiety was introduced by attaching 3-(2-pyridyldithio)propionic acid[21] *via* amide coupling reactions to the focal point of the dendritic structure. We investigated a synthetic pathway for the dendritic molecular transporter in which the pyridinyldithio moiety is attached to the focal point of the dendrimer, **4**, at an early step in the synthetic pathway that was started from the G1 Newkome dendrimer, **1** (Scheme 1). The amine group was transformed with 3-(2-pyridyldithio)propionic acid *via* amide coupling reaction to yield compound **2** after a subsequent deprotection of the *tert*-butyl end group functionalities with formic acid. The peripheral carboxylic acid groups were reacted with *N*-Boc-1,6-diaminohexane through amide coupling, and the Boc groups on the resulting products were then deprotected with 2 M HCl in 1,4-dioxane to yield the amine salt, **3**. The guanidinylation of the free amine groups with *N,N′*-di-Boc-*N′′*-triflylguanidine furnished the molecular transporter building block, **4**, that was utilized to further refine and post-modify polymeric nanoparticles for the delivery of peptidic molecules into cells.

To provide biocompatible scaffolds with the ability to transport higher drug loads, we proposed the utilization of coiled and cross-linked linear hydrophilic polymers resembling protein structures. These nanoobjects have a size dimension of 5−10 nm, the smallest diameters known for polymeric structures assembled from linear polymers.[15,16] The ideal nanoscopic size dimension under 25 nm together with the ability of systematic modification of these nanoobjects will have tremendous impact on the allocation of scaffolds with biological activity. We have developed a synthetic pathway to incorporate orthogonal functionalities which will allow for the conjugation of the molecular transporter building block and therapeutics. The synthesis of the delivery system started with the conjugation of

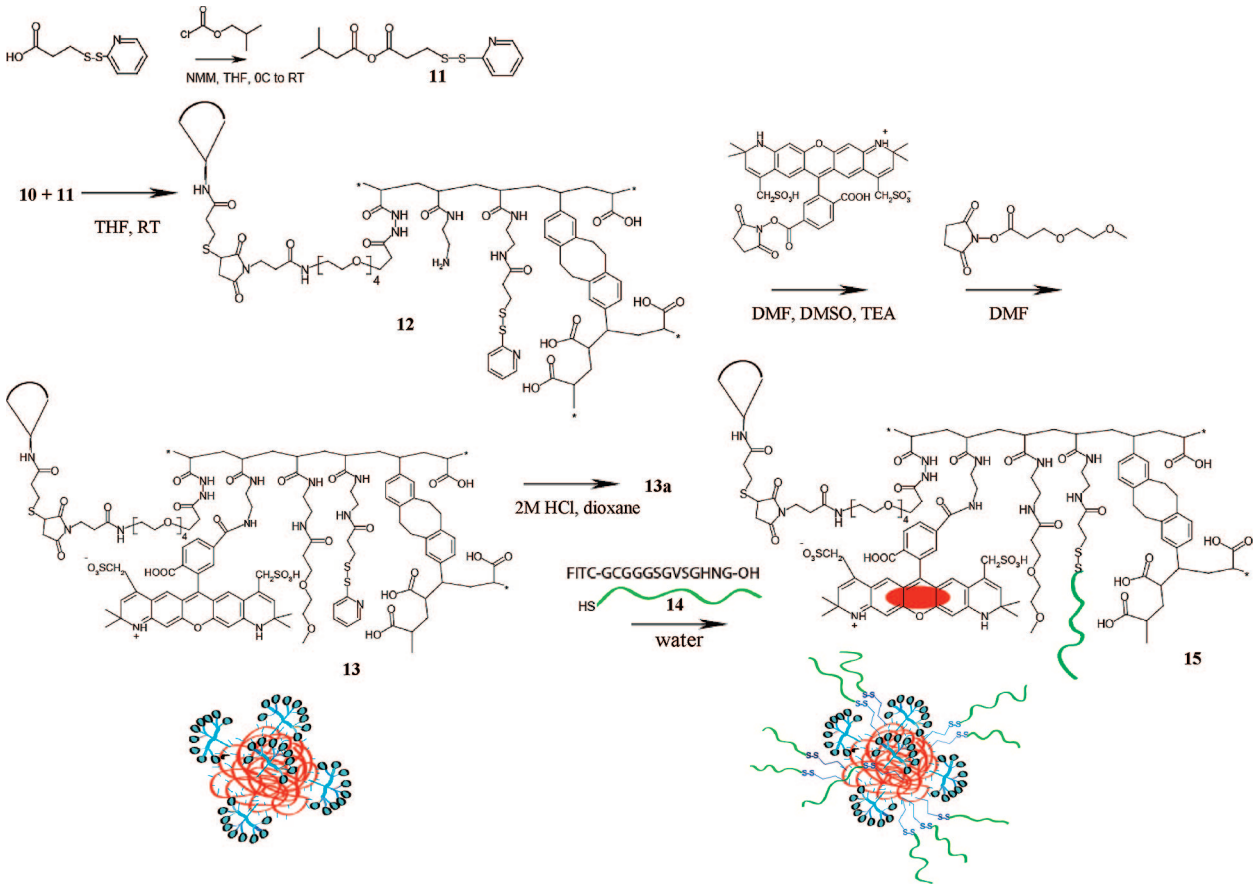

Scheme 3. Synthesis of nanoparticle conjugates modified with molecular transporter, disulfide linker, and dye 13 and after disulfide exchange reaction to yield nanoparticle−peptide−molecular transporter−dye conjugate 15.

a *N*-Tfa-ethylenediamine linker to chloroformate activated carboxylic acids on the nanoparticle *via* amide coupling reactions. The quantity of the base labile protected linker can be varied according to the intended amount of biological drug load per particle. Although the nanoparticles are coiled and cross-linked, the low cross-linking density allows for soluble macromolecular structures that can be analyzed by NMR spectroscopy. After the attachment of *N*-Tfa-ethylenediamine to the particles, we subsequently conjugated maleimide-dPEG$_4$-hydrazide linker to other present carboxylic acids on the particles *via* amide coupling reactions to give compound **7** (Scheme 2). The maleimide functionality serves as the conjugation site for the thiol group originated from molecular transporter's focal point. Therefore, prior to the conjugation of the protected molecular transporter, **4**, a reductive cleavage of the disulfide linker with dithiolthreitol (DTT) is necessary to form the free thiol unit that reacts with the maleimide in DMF, covalently attaching the transporter, **8**, to the nanoparticle backbone. After purification through dialysis, we determined that 10 molecular transporter molecules were conjugated to the estimated 15 available maleimide units according to the NMR spectroscopy data analysis. The synthesis continued with the deprotection of the trifluoroacetyl-protected amines conjugated to the nanoparticle backbone, and we found that potassium carbonate (K_2CO_3) in methanol and water at room temperature gave the best results to achieve a complete deprotection of the amine groups without cleaving the Boc groups on the peripheral guanidine functionalities. The purification of the nanoparticle conjugates can be performed in either methanol or THF depending on the solubility of conjugate products and can simplify the overall synthesis. In a following modification step, chloroformate-activated 3-(2-pyridyldithio)propionic acid (PDPOH), **11**, was attached to the available amine functionalities resulting from the deprotected *N*-Tfa-ethylenediamine linker. The high efficiency of this reaction allows for a stoichiometrically controlled modification with a specific amount of linkers to the particles so that all of the amines can be reacted with PDPOH or as to leave some free amines still available for the attachment of other units such as a fluorophore. This fact underlines the great variability of the chemistry and the control exhibited in proceeding modification steps. In view of the planned disulfide exchange reaction with cysteine units in peptides, approximately 45 amine groups were modified with the disulfide linker PDPOH, and the remaining amine groups were available for the attachment of the fluorophore (see Supporting Information). Therefore, to moni-

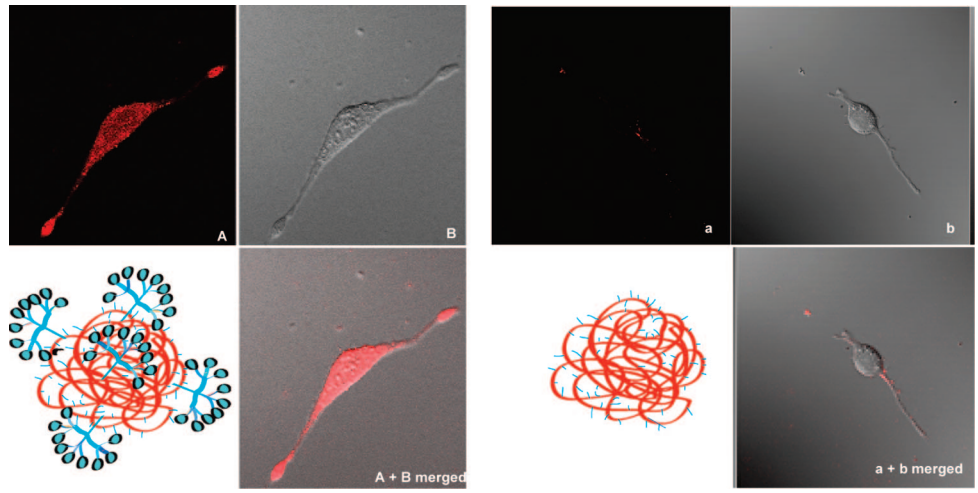

Figure 1. Cellular uptake experiments of nanoparticle−transporter conjugate 13a into NIH 3T3 cells investigated *via* confocal microscopy. The cells were incubated for 30 min with a 4 μM solution of 13a in Hanks buffered saline solution (HBSS). (A) Imaged for the red fluorescence of the Alexa Fluor 568 and (B) DIC image of cell; (a) negative control of nanoparticle 6a labeled with Alexa Fluor 568 and (b) DIC image of cell. The cells were incubated for 30 min with a 4 μM solution of 6a in Hanks buffered saline solution (HBSS).

tor the uptake and cellular localization of the nanoparticle scaffold of the nanoparticle−molecular transporter−peptide conjugate, we attached NHS ester activated Alexa Fluor 568 to approximately 20 of the remaining free amine groups. Amine entities that were not modified with dye or linker were subsequently capped using NHS-m-dPEG.

Ultimately, the Boc protecting groups on the dendritic molecular transporter were successfully deprotected using 2 M HCl in 1,4-dioxane to reveal the free guanidinyl end groups of the attached dentritic transporter (Scheme 3). As previously mentioned, the amount of pyridinyldithio moiety attached to the nanoparticle determines the number of peptide units or therapeutics that can be conjugated to the particle *via* thiol−disulfide exchange reactions. Therapeutic cargo such as peptides or oligonucleotides must contain a sulfhydryl functionality to afford the exchange reaction, which facilitates a disulfide bond to introduce the therapeutic cargo to the particles for release of the cargo from the carrier in a reductive environment. We conjugated fluorescein isothiocyanate (FITC)-labeled peptides (FITC-GG-13), **14**, to the nanoparticles *via* thiol−disulfide exchange reaction under aqueous reaction conditions. To evaluate the amount of peptides attached as a result of the exchange reaction, we could not rely on NMR spectroscopy because characteristic peaks were not isolated and could not be selected as internal standards. Therefore, the absorbance properties were inspected for a sign of analytical utility. The NanoDrop method allows measuring the absorbance of approximately 2 μL droplets of conjugate solution. The method of multiple standard addition was performed using a known concentration of peptide as the sample spike to a solution composed from a known mass of nanoparticle conjugate **15** in a known volume. This method includes the assumption that the molar absorptivity of the peptide does not change when conjugated to the nanoparticles because absorbing species are not significantly modified. After peptide aliquot additions, standard addition curves were generated for all wavelengths with a significant signal from either the peptide or the conjugate (238, 280, 320, 493 nm). The amount of conjugated peptide in the nanoparticle conjugate **15** solution was found to be approximately the same for each wavelength with 24 peptides conjugated, which corresponds to a 30% drug load of the delivery system (see Supporting Information).

We investigated the uptake behavior of the assembled macromolecular structures, both the Alexa Fluor 568 labeled nanoparticles before peptide conjugation, **13a**, and the nanoparticle−peptide conjugate, **15**, with NIH 3T3 mouse fibroblast cells. The nanoparticle conjugates were solubilized in water and diluted with Hanks buffered saline solution (HBSS) to the desired concentration of material. The cells were then incubated at 37 °C with the nanoparticle conjugate solution for 30 min and then washed with HBSS supplemented with 5 mM glucose and imaged *via* confocal microscopy. First, we investigated the uptake of the Alexa Fluor 568 dye labeled nanoparticle−transporter conjugates, **13a**, and observed a strong red fluorescence in the 3T3 cells as seen in Figure 1A. A negative control experiment with nanoparticles, **6a**, with only Alexa Fluor 568 dye but no transporter conjugated to the backbone, did not enter the cells (Figure 1a). It is evident that the conjugated transporter is a critical attribute to facilitate efficient and rapid uptake of the nanoparticle across the cellular membranes. In the next experiment, cells incubated with the prepared peptide delivery system, nanoparticle−peptide conjugate **15**, were imaged for

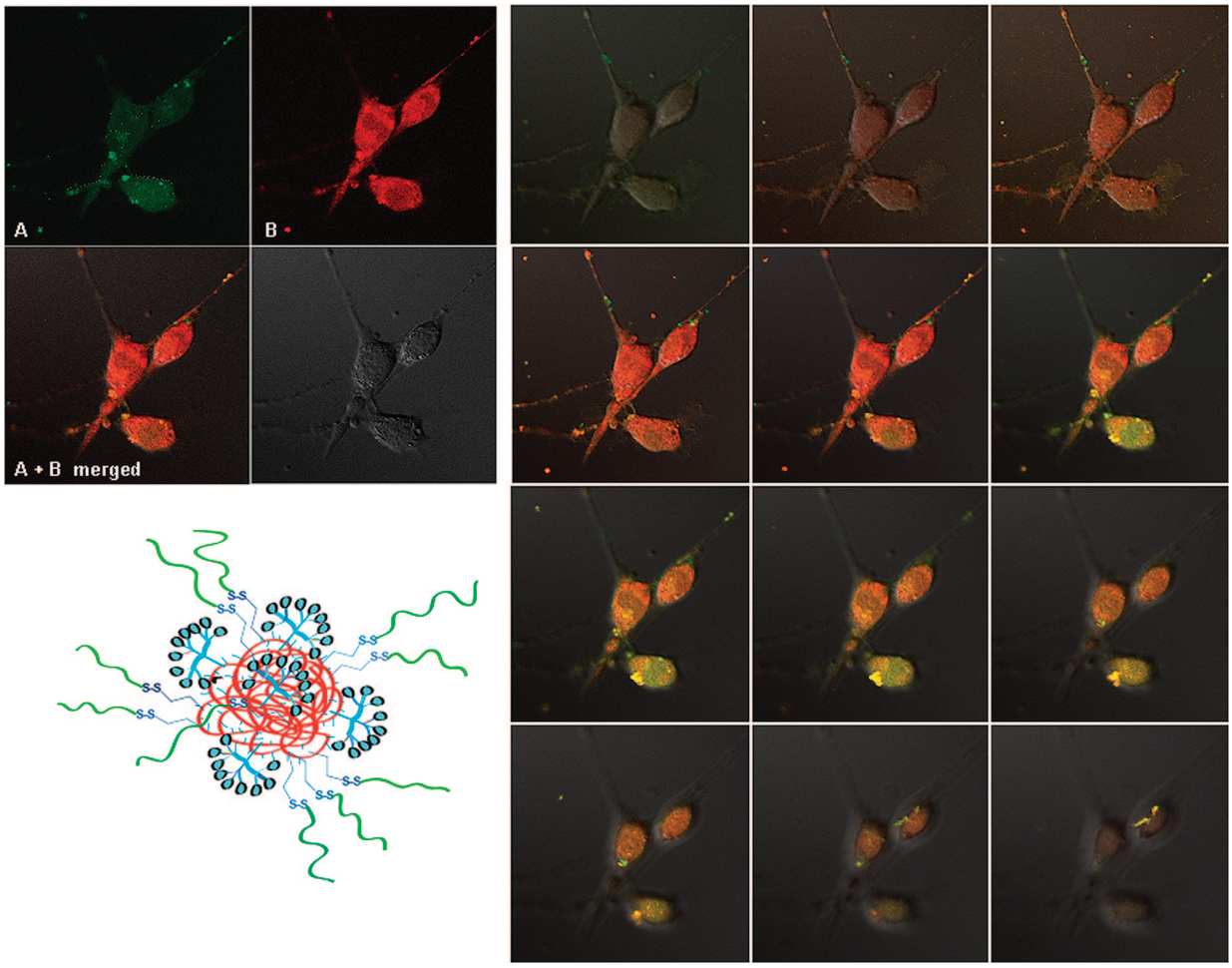

Figure 2. Cellular uptake experiments of nanoparticle−transporter conjugate 15 into NIH 3T3 cells investigated *via* confocal microscopy imaged for the fluorescence of the Alexa Fluor 568 dye (B) and the fluorescein (A), with complementing *z*-stack showing the presence of both fluorophores from the bottom (top, left) to the top of the cells (bottom, right). The cells were incubated for 30 min with a 37.2 μM solution of 15 in Hanks buffered saline solution (HBSS).

emission wavelengths of the Alexa Fluor 568 dye, labeling the particle backbone and the fluorescein dye, the marker of the peptide. We detected the presence of both of the fluorophores inside the cells, indicating the efficient uptake and transport of the conjugate across the cellular membrane (Figure 2A,B). The initial investigation of the *z*-stack suggested a cleavage of the peptides from the carriers being in progress, with the red fluorescence observed more intensely in the bottom layers than the ones from the above layers of the cells (Figure 2). Since FITC is more susceptible for photobleaching than Alexa Fluor dye, the cleavage of the peptide might be more obvious with other more stable dyes. Another method to actually quantitate the amount of peptide delivered into the cells will be investigated in further detail in future experiments. Nevertheless, it is evident that these cellular uptake experiments demonstrate the uptake of organic, high molecular weight hydrophilic nanoparticle−therapeutic conjugates with a similar molecular weight as proteins and antibodies of around 130 kDa with the promotion of the developed dendritic molecular transporter attached. These nanocarrier systems are poised to also serve as a powerful delivery platform of other relevant and precious biological cargos with the need of rapid uptake into cells.

In conclusion, we have further demonstrated the utilization of developed dendritic molecular transporter in the assembly of a novel delivery system with cross-linked coiled nanoparticles in a protein inspired design to form a carrier that rapidly transports multiple copies of peptide units per particle across the cellular barrier into the cytoplasm of 3T3 cells. Sequential attachment strategies together with the versatility of the architectural design of the carrier allow for the adjustment of peptide drug loads through variable amounts of integrated disulfide linker that facilitate the cleavage and release in the cell. The uptake experiments into 3T3 cells showed that the dendritic molecular transporter unit is critical for the intracellular delivery. The developed unique synthetic platform can be extended to the delivery of other therapeutics such as siRNA and other cargo that require a rapid and unaltered delivery to unfold its biological activity.

EXPERIMENTAL METHODS

Materials: All reagents were purchased either from AAPER Alcohol and Chemical Co. (Shelbyville, KY), Acros Organics, Alfa Aesar, EMD, Fisher, Invitrogen (Carlsbad, CA), J.T. Bakker, Lonza (Walkersville, MD), or Sigma-Aldrich and used without further purification unless otherwise noted. Analytical TLC was performed on commercial Merck plates coated with silica gel 60 F_{254} and spots located by UV light (254 and 366 nm). Silica gel for flash chromatography was obtained from Sorbent Technologies (60 Å, 230−400 mesh). MAL-dPEG$_4$-*t*-Boc-hydrazide and NHS-mdPEG were obtained from Quanta Biodesign, Ltd. (Powell, OH) and used as received. Alexa Fluor 568 was purchased from Molecular Probes (Eugene, OR). FITC-labeled GG peptide (FITC-GCGGGSGVSGHNG-OH), **14**, was obtained from GL Biochem Ltd. (Shanghai, China). Spectra/Por Biotech Cellulose Ester (CE) Dialysis Membranes (1000 MWCO) were obtained from Spectrum Laboratories, Inc. (Rancho Dominguez, CA). SnakeSkin Pleated Dialysis Tubing (10 000 MWCO) was obtained from Pierce Biotechnology, Inc. (Rockford, IL). Amicon Ultra centrifugal filter devices (10 000 MWCO) were obtained from Millipore Co. (Billerica, MA). Nanoparticles were synthesized according to the previously published procedures, with the benzyl acrylate nanoparticles undergoing an additional purification *via* flash column chromatography, eluting with hexanes, and increasing to 100% ethyl acetate to give light yellow nanoparticles.

Instrumentation: Nuclear magnetic resonance was performed on a Bruker DPX-300, a Bruker AV-400, Bruker DRX-500, or Bruker AV-II spectrometer. Chemical shifts are reported in parts per million and referenced to the corresponding residual nuclei in deuterated solvents. Gel permeation chromatography was performed in tetrahydrofuran (THF) with the eluent at a flow rate of 1 mL/min on a Waters chromatograph equipped with four 5 mm Waters columns (300 mm × 7.7 mm) connected in series with increasing pore size (100, 1000, 100 000, and 1 000 000 Å, respectively). A Waters 2487 dual λ absorbance detector and a 2414 refractive index detector were employed. Dynamic light scattering was performed on a Malvern Zetasizer Nanoseries instrument with a CGS-3 compact goniometer system. Uncoated, 14 mm diameter Microwell, No. 1.5 MatTek dishes were purchased from MatTek Corp. (Ashland, MA). UV−vis measurements were performed on a NanoDrop 1000 spectrophotometer.

Modification of Nanoparticles. ***Synthesis of N-Boc-N-Tfa-ethylenediamine.*** *N*-Boc-ethylenediamine (5.0 g, 31.2 mmol) in THF (20 mL) was stirred at 0 °C; ethyl trifluoroacetate (3.72 mL, 31.2 mmol) was added dropwise and the reaction stirred overnight. The reaction solution was concentrated to yield a white crystalline product (8.0 g, 99%): ^{1}H NMR (400 MHz, $CDCl_3$) δ 7.85 (s, 1H, NH), 5.01 (s, 1H, NH), 3.46 (dd, 2H, J = 5.1, 10.4 Hz, CH_2), 3.37 (dd, 2H, J = 5.4, 10.2 Hz, CH_2), 1.44 (s, 9H, CH_3); ^{13}C NMR (400 MHz, $CDCl_3$) δ 157.7, 151.2, 140.6, 80.6, 42.2, 39.1, 28.2.

Boc Deprotection of N-Boc-N-Tfa-ethylenediamine. *N*-Boc-*N*-Tfa-ethylenediamine (8.0 g, 31.5 mmol) was dissolved in 50 mL of formic acid and stirred for 14 h at room temperature. After the solvent was evaporated under reduced pressure, toluene was added and concentrated to remove any residual formic acid, yielding an orange oil (4.90 g, 99%): ^{1}H NMR (400 MHz, MeOD) δ 8.35 (s, 1H, NH), 3.61 (t, 2H, J = 6.1 Hz, CH_2), 3.15 (t, 2H, J = 6.1 Hz, CH_2), 2.31 (s, 2H, NH_2); ^{13}C NMR (400 MHz, MeOD) δ 160.1, 159.7, 121.6, 118.8, 115.9, 113.1, 39.7, 38.5.

***Attachment of N-Tfa-ethylenediamine,* 6.** The carboxylic acid nanoparticles **5** (162.3 mg, 4.58 μmol) in DriSolv DMF (10.0 mL) were stirred under argon at 0 °C with *N*-methylmorpholine (47.8 mg, 472.6 μmol) followed by dropwise addition of isobutyl chloroformate (71.0 mg, 519.8 μmol) in DriSolv DMF (0.75 mL). After 1.5 h, a solution of *N*-Tfa-ethylenediamine (73.8 mg, 472.6 μmol) in DriSolv DMF (2.5 mL) was added dropwise. The reaction was allowed to warm to room temperature and stirred overnight. After removal of DMF *in vacuo*, the product was dissolved in methanol and dialyzed against methanol with SnakeSkin Pleated Dialysis Tubing (10 000 MWCO; 141 mg, 68%): ^{1}H NMR (400 MHz, MeOD) δ 7.29−6.82 (114H, br m, ArH), 2.99 (40H, br s, C*H*$_2$NH), 2.83−2.74 (97H, br m, CH_2NH, CH_2), 2.34−1.61 (852H, br m, CH_2). The significant change is the appearance of two broad resonance peaks at 2.74−2.83 and 2.99−3.01 ppm due to the trifluoroacetyl-protected diamine; otherwise, all other aspects of the spectrum are similar.

Deprotection of MAL-dPEG$_4$-t-Boc-hydrazide. In a 100 mL round-bottomed flask, MAL-dPEG$_4$-*t*-Boc-hydrazide (127.1 mg, 239.5 μmol) was dissolved in 80.0 mL of formic acid and stirred overnight at room temperature. After the solvent was evaporated under reduced pressure, toluene was added and concentrated to remove any residual formic acid to give MAL-dPEG$_4$-hydrazide (103 mg, 100%).

***Attachment of MAL-dPEG$_4$-hydrazide,* 7.** The nanoparticles **6** (141.1 mg, 3.13 μmol) in DriSolv DMF (10.0 mL) were stirred under argon at 0 °C with *N*-methylmorpholine (17.1 mg, 169.1 μmol) followed by dropwise addition of isobutyl chloroformate (25.4 mg, 86.0 μmol) in DriSolv DMF (0.7 mL). After 1.5 h, a solution of MAL-dPEG$_4$-hydrazide (103.1 mg, 239.5 μmol) was added dropwise. The reaction was allowed to warm to room temperature and stirred overnight. After removal of DMF *in vacuo*, the product was dissolved in MeOH and dialyzed against MeOH with SnakeSkin Pleated Dialysis Tubing (10 000 MWCO; 147 mg, 88%): ^{1}H NMR (400 MHz, MeOD) δ 8.08−6.72 (126H, br m, ArH, CH, NH), 3.67−3.41 (244H, br m, CH_2OCH_2), 2.98 (71H, br s, C*H*$_2$NH), 2.89−2.76 (195H, br m, CH_2NH, CH_2), 2.44−1.61 (1107H, br m, CH_2). The significant change is the appearance of broad resonance peaks at 3.41−3.67 and 7.98−8.08 ppm and a resonance peak at 6.72 ppm due to the MAL-dPEG$_4$-hydrazide; otherwise, all other aspects of the spectrum are similar.

***Cleavage of Disulfide Bridge on Molecular Transporter,* 8.** The disulfide linker hexyl molecular transporter **4** (257.8 mg, 61.4 μmol) in DriSolv DMF (5 mL) was stirred under argon, and a solution of DL-dithiothreitol (740.0 mg, 4.80 mmol) in DMF (5 mL) was added dropwise, and the reaction proceeded for 2 h at room temperature. After removal of DMF *in vacuo*, the reaction was purified using a Sephadex LH-20 column, eluting with DMF and concentrating the fractions *in vacuo*, again yielding the product (251 mg, 100%).

***Attachment of Molecular Transporter,* 9.** The nanoparticles **7** (147.4 mg, 3.07 μmol) in DriSolv DMF (10.0 mL) were stirred under argon, and the free thiol hexyl molecular transporter (251.0 mg, 61.4 μmol) in DriSolv DMF (10.0 mL) was added dropwise followed by the addition of a catalytic amount of *N*-methylmorpholine, and the reaction proceeded overnight. After removal of DMF *in vacuo*, the product was dissolved in methanol and dialyzed against a 1:1 MeOH/H_2O solution, eventually dialyzing against pure methanol with SnakeSkin Pleated Dialysis Tubing (10 000 MWCO; 142 mg, 54%): ^{1}H NMR (400 MHz, MeOD) 8.37−6.80 (400H, br m, ArH), 3.68−3.41 (244H, br m, CH_2OCH_2), 3.06−2.99 (253H, br m, CH_2, C*H*$_2$NH), 2.83−2.66 (333H, br m, CH_2, CH_2NH), 2.34−1.19 (3496H, br m, CH_3, CH_2). The significant change is the appearance of a broad resonance peaks at 1.28, 1.37, 1.42, 1.87, 2.07, 2.83, and 3.06 ppm and the disappearance of the peak at 6.72 ppm due to the hexyl molecular transporter; otherwise, all other aspects of the spectrum are similar.

***Deprotection of Trifluoroacetyl-Protected Amines,* 10.** The nanoparticles **9** (141.9 mg, 1.54 μmol) were dissolved in MeOH (5.0 mL), and a 10% K_2CO_3 solution of 5:3 MeOH/H_2O (13.0 mL) was added to the solution, and the reaction proceeded overnight at room temperature. The reaction was purified by dialysis with SnakeSkin Pleated Dialysis Tubing (10 000 MWCO) against a 5:3 MeOH/H_2O solution, eventually dialyzing against pure MeOH then dialyzing against a 1:1 MeOH/THF solution, eventually dialyzing against pure THF (111 mg, 84%): ^{1}H NMR (400 MHz, THF-d_8) δ 8.36−7.10 (292H, br m, ArH, NH), 3.82−3.79 (244H, br m, CH_2OCH_2), 3.51−3.33 (200H, br m, CH_2, CH_2NH), 3.27−3.14 (173H, br m, CH_2, C*H*$_2$NH), 2.57−1.29 (5236H, br m, CH_3, CH_2, NH_2). The significant change is the appearance of a broad resonance peak at 2.57 ppm due to the free amine; otherwise, all other aspects of the spectrum are similar.

***Attachment of 3-(2-Pyridyldithio)propionic acid,* 12.** A solution of 3-(2-pyridyldithio)propionic acid (16.8 mg, 77.9 μmol) in anhydrous THF (2.5 mL) was stirred under argon at 0 °C with *N*-methylmorpholine (7.88 mg, 77.9 μmol), followed by dropwise addition of isobutyl chloroformate (11.7 mg, 85.7 μmol) to form **11** *in situ*. After 1.5 h, a solution of the nanoparticles **10** (111.0 mg, 1.30 μmol) in anhydrous THF (35.0 mL) was added

dropwise. The reaction was allowed to warm to room temperature and stirred for 24 h. The reaction was diluted and purified by dialysis with SnakeSkin Pleated Dialysis Tubing (10 000 MWCO) against MeOH, eventually dialyzing against a 3:1 THF/MeOH solution (98 mg, 80%): ^{1}H NMR (400 MHz, THF-d_8) δ 8.47−6.59 (821H, br m, ArH, NH), 4.09−3.97 (244H, br m, CH_2OCH_2), 3.47 (45H, br t, CH_2), 3.36−3.35 (269H, br m, CH_2, CH_2NH), 3.14 (281H, br s, CH_2, CH_2NH), 2.97−1.09 (18596H, br m, CH_3, CH_2, NH_2). The significant change is the appearance of a broad multiplet resonance peak at 3.47 ppm and an increase in the signal in the aromatic region due to PDPOH; otherwise, all other aspects of the spectrum are similar.

Attachment of Alexa Fluor 568. To a solution of multifunctional nanoparticles **12** (5.0 mg, 53.0 nmol) in DriSolv DMF (1.25 mL), was added a solution of Alexa Fluor 568 (2.58 mg, 3.26 μmol) in anhydrous DMSO (258.1 μL) and triethylamine (25.0 μL, 179.4 μmol), and the reaction proceeded in the dark for 24 h at room temperature.

Capping of the Remaining Amines, 13. Upon completion of the Alexa Fluor 568 addition to the nanoparticles, a solution of NHS-m-dPEG (2.99 mg, 12.2 μmol) in DriSolv DMF (600 μL) was added to the reaction solution. The reaction was allowed to proceed for 10 h at room temperature and was then diluted with MeOH and purified by dialysis with SnakeSkin Pleated Dialysis Tubing (10 000 MWCO) dialyzing against MeOH, eventually dialyzing against a 1:1 MeOH/H_2O solution (4.53 mg, 79%): ^{1}H NMR (600 MHz, D_2O) δ 8.84−5.72 (br m, ArH, NH), 4.33−3.51 (br m, CH_2OCH_2, SO_2OH), 3.51−3.00 (br m, CH_2, CH_2NH), 3.00−1.08 (br m, CH_3, CH_2, NH). The significant changes are the increase in signal of the broad resonance peak at 3.00−1.08 due to NHS-m-dPEG and Alexa Fluor 568, the increase in signal of the broad resonance peak at 4.33−3.51 ppm due to NHS-m-dPEG, and an increase in the signal in the aromatic region due to Alexa Fluor 568; otherwise, all other aspects of the spectrum are similar.

Boc Deprotection 13a. Modified nanoparticles, **13** (4.53 mg, 41.7 nmol) were dissolved in anhydrous 1,4-dioxane (6.0 mL) and chilled to 0 °C. A solution of 4 M HCl in 1,4-dioxane (6.0 mL) was added dropwise to the stirring nanoparticles, and the reaction was allowed to proceed overnight at room temperature. The nanoparticle solution was diluted to three times the original volume with H_2O and dialyzed against H_2O with SnakeSkin Pleated Dialysis Tubing (10 000 MWCO). Upon completion of dialysis, the aqueous solution was concentrated to give a bright pink product (3.25 mg, 86%): ^{1}H NMR (600 MHz, D_2O) δ 8.61−6.86 (br m, ArH, NH), 4.09−3.34 (br m, CH_2OCH_2, SO_2OH), 3.34−2.58 (br m, CH_2, CH_2NH), 2.5−0.41 (br m, CH_3, CH_2, NH, NH_2). The significant change is the decrease in signal and the disappearance of two broad resonance peaks in the aliphatic region due to the removal of the *tert*-butoxycarbonyl protecting groups on the molecular transporter; otherwise, all other aspects of the spectrum are similar.

***GG Peptide Attachment,* 15.** A solution of modified nanoparticles (MFNP) **13a** (2.0 mg, 22.1 nmol) in H_2O (540.5 μL) was added to a solution of FITC-labeled GG peptide (FITC-GG-13) (1.85 mg, 1.19 μmol) in H_2O (0.5 mL), followed by the addition of 3.36 mL of H_2O, and the reaction was stirred overnight at room temperature. The reaction was then diluted with H_2O and dialyzed against H_2O with SnakeSkin Pleated Dialysis Tubing (10 000 MWCO). Upon completion of dialysis, the aqueous solution was concentrated to give an orange conjugate (2.66 mg, 96%): ^{1}H NMR (600 MHz, D_2O) δ 8.89−6.08 (br m, ArH, NH), 4.57−3.34 (br m, CH_2OCH_2, CH, CH_2, CH_2S, CH_2OH, SO_2OH), 3.34−2.54 (br m, CH_2, CH_2NH), 2.54−0.40 (br m, CH_3, CH_2, $CH(CH_3)_2$, NH, NH_2). The significant change is the increase in signal and the appearance of sharper peaks in all regions due to the peptide; otherwise, all other aspects of the spectrum are similar.

Control Particle Synthesis. After the attachment of *N*-Tfa-ethylenediamine to carboxylic acid nanoparticles, **6**, and subsequent workup, a portion of the modified particles (15.0 mg, 342.0 μmol) in MeOH (528.5 μL) was deprotected using a 10% K_2CO_3 solution of 5:3 MeOH/H_2O (1.38 mL) and purified as described above (12.1 mg, 88%).

Attachment of Alexa Fluor 568, 6a. To the deprotected nanoparticles of the previous reaction (5.0 mg, 124.9 nmol) in DMF (1.03 mL) was added a solution of Alexa Fluor 568 NHS ester dye (3.96 mg, 5.0 μmol) in anhydrous DMSO (395.6 μL) and triethylamine (25 μL, 179.4 μmol), and the solution was diluted with 71.2 μL of DMF. The reaction proceeded in the dark for 24 h at room temperature and the remaining amines were then capped with NHC-m-dPEG as reported above. The solution was diluted with H_2O and purified *via* centrifugation with Amicon Ultra centrifugal filter devices (10 000 MWCO) rinsing with H_2O (470 μg, 7%): ^{1}H NMR (600 MHz, D_2O) δ 8.43−6.92 (br m, ArH, NH), 3.80−3.62 (br m, CH_2OCH_2, SO_2OH), 3.39−3.31 (br m, CH_2NH), 2.58−1.01 (br m, CH_3, CH_2, NH). The significant changes are the increase in signal of the broad resonance peak at 3.80−3.62 due to NHS-m-dPEG and Alexa Fluor 568, the increase in signal of the broad resonance peak, and an increase in the signal in the aromatic region due to Alexa Fluor 568; otherwise, all other aspects of the spectrum are similar.

Cell Culture and Nanoparticle Cell Uptake by Confocal Laser Scanning Microscopy (CLSM). NIH 3T3 mouse fibroblast cells (ATCC CCL-1658, American type Culture Collection) were grown in Dubelco's modified eagle medium (DMEM, ATCC, 30-2002) supplemented with 10% calf serum (ATCC) and 1% antibiotic-antimycotic (Invitrogen, 15240) at 37 °C with 5% CO_2 in a 95% humidity incubator.

Confocal microscopy was performed using a Zeiss Inverted LSM 510 Meta laser scanning confocal microscope, equipped with an argon laser, a 543 nm HeNe laser, a Plan-Neofluar 40×/1.3 oil lens and a Plan-Apochromat 63×/1.4 oil lens. Samples were analyzed using three-channel confocal laser scanning microscopy to obtain a DIC image combined with FITC and Alexa Fluor 568 fluorescence images. The 3T3 cells were plated on uncoated, 14 mm diameter Microwell, No. 1.5 MatTek dishes at a density of 2.5×10^5 cells per well in medium. On the day of experiments, cells were washed with prewarmed Hank's buffered saline solution (HBSS) with Ca^{2+} and Mg^{2+} (Gibco, Grand Island, NY) supplemented with 5 mM glucose and incubated with HBSS for 1 h before adding nanoparticles or conjugates. Cells were then treated with 100 μL of the negative control particles **6a** (4.0 μM conjugate), fluorescent nanoparticles **13a** (4.0 μM conjugate = 40 μM molecular transporter), or fluorescent bioconjugate **15** (MFNP+GG) (37.2 μM conjugate = 372.3 μM molecular transporter) for the incubation times, washed twice with HBSS without Ca^{2+} and Mg^{2+} (Gibco, Grand Island, NY), and fed with HBSS with Ca^{2+} and Mg^{2+} supplemented with 5 mM glucose for visualization by confocal microscopy. Imaging was performed on a Zeiss LSM 510 META confocal microscope through the use of the VUMC Cell Imaging Shared Resource (supported by NIH Grants CA68485, DK20593, DK58404, HD15052, DK59637, and EY08126).

NanoDrop Analysis: By utilizing a NanoDrop spectophotometer, we were able to obtain UV−vis measurements on very small (2 μL) volumes of solutions to perform a standard addition method by adding a known amount of peptide **14** to an unknown solution. Standard addition curves were generated for each of the measured wavelengths, and the amount of peptide and nanoparticles in our unknown solution was calculated. The amount of conjugated peptide in the unknown solution was found to be approximately the same for each wavelength, thus confirming the accuracy of this method.

A 100 μM solution of FITC-GG-13 peptide **14** and a 0.3 mg/mL solution of dye-MFNP-GG conjugate **15** were made up in cell culture water (Lonza, Walkersville, MD). The absorbency of the conjugate **15** solution was measured and recorded using the UV−vis mode of a NanoDrop 1000 spectrophotometer at wavelengths of 238, 280, 320, and 493 nm, where there was significant signal from the peptide **14** and the conjugate **15**. Ten or 20 μL aliquots of 100 μM peptide **14** solution were added sequentially to the conjugate **15** solution, with absorbency measurements being taken after each aliquot addition at wavelengths of 238, 280, 320, and 493 nm. Upon completing 12 aliquot additions, the known peptide **14** concentrations were plotted against the recorded absorbencies for each wavelength and linear trend lines rendered (see Supporting Information). Extrapolating the trend line to the *y*-axis intercept, by setting the *y* value in the trend line equation to 0, gave the peptide **14** concentration of the originally measured **15** conjugate solution. The peptide **14** concentration was then converted into milligrams of peptide, and this number was used to calculate the

amount of dye-MFNP **13a** in the originally measured conjugate **15** solution. The moles of peptide **14** can then be normalized by the moles of dye-MFNP **13a** to give an average of 24 peptides **14** per dye-MFNP **13a**. Propagation of error with 95% certainty was calculated to be $\pm 2.88 \times 10^{-6}$ for absorbency at 238 and 280 nm, $\pm 4.22 \times 10^{-6}$ for absorbency at 320 nm, and $\pm 3.82 \times 10^{-6}$ for absorbency at 493 nm.

Acknowledgment. The authors would like to thank Vanderbilt University (VINSE, Vanderbilt Institute of Nanoscale Science and Engineering) and the Vanderbilt Institute of Chemical Biology (VICB, pilot grant), and the National Science Foundation NSF (CHE 0645737) for supporting this research. We would like to thank Prof. K. Sam Wells, Vanderbilt Imaging Core VUMC, for valuable discussions regarding live cell imaging studies, and Prof. Frederick R. Haselton, Department of Biomedical Engineering, for training of S.K.H. to perform cell studies.

Supporting Information Available: Characterization and analysis of nanoparticle conjugates. This material is available free of charge *via* the Internet at http://pubs.acs.org.

REFERENCES AND NOTES

1. Ferrari, M. Cancer Nanotechnology: Opportunities and Challenges. *Nat. Rev. Cancer* **2005**, *5*, 161–171.
2. Torchilin, V. P.; Levchenko, T. S. Tat-Liposomes: A Novel Intracellular Drug Carrier. *Curr. Protein Pept. Sci.* **2003**, *4*, 133–140.
3. Belting, M.; Sandgren, S.; Wittrup, A. Nuclear Delivery of Macromolecules: Barriers and Carriers. *Adv. Drug Delivery Rev.* **2005**, *57*, 505–527.
4. Goun, E. A.; Pillow, T. H.; Jones, L. R.; Rothbard, J. B.; Wender, P. A. Molecular Transporters: Synthesis of Oligoguanidinium Transporters and Their Application to Drug Delivery and Real-Time Imaging. *ChemBioChem* **2006**, *7*, 1497–1515.
5. Wender, P. A.; Galliher, W. C.; Goun, E. A.; Jones, L. R.; Pillow, T. H. The Design of Guanidinium-Rich Transporters and Their Internalization Mechanisms. *Adv. Drug Delivery Rev.* **2008**, *60*, 452–472.
6. Zhang, K.; Fang, H.; Chen, Z.; Taylor, J.-S. A.; Wooley, K. L. Shape Effects of Nanoparticles Conjugated with Cell-Penetrating Peptides (HIV Tat PTD) on CHO Cell Uptake. *Bioconjugate Chem.* **2008**, *19*, 1880–1887.
7. Wender, P. A.; Kreider, E.; Pelkey, E. T.; Rothbard, J.; VanDeusen, C. L. Dendrimeric Molecular Transporters: Synthesis and Evaluation of Tunable Polyguanidino Dendrimers That Facilitate Cellular Uptake. *Org. Lett.* **2005**, *7*, 4815–4818.
8. Okuyama, M.; Laman, H.; Kingsbury, S. R.; Visintin, C.; Leo, E.; Eward, K. L.; Stoeber, K.; Boshoff, C.; Williams, G. H.; Selwood, D. L. Small-Molecule Mimics of an Alpha-Helix for Efficient Transport of Proteins into Cells. *Nat. Methods* **2007**, *4*, 153–159.
9. Maiti, K. K.; Jeon, O. Y.; Lee, W. S.; Chung, S. K. Design, Synthesis, and Delivery Properties of Novel Guanidine-Containing Molecular Transporters Built on Dimeric Inositol Scaffolds. *Chem.—Eur. J.* **2007**, *13*, 762–775.
10. Huang, K.; Voss, B.; Kumar, D.; Hamm, H. E.; Harth, E. Dendritic Molecular Transporters Provide Control of Delivery to Intracellular Compartments. *Bioconjugate Chem.* **2007**, *18*, 403–409.
11. Foerg, C.; Merkle, H. P. On the Biomedical Promise of Cell Penetrating Peptides: Limits *versus* Prospects. *J. Pharm. Sci.* **2008**, *97*, 144–162.
12. Hamilton, S. K.; Ikizler, M. R.; Wallen, C.; Wright, P. F.; Harth, E. Effective Delivery of IgG-Antibodies into Infected Cells *via* Dendritic Molecular Transporter Conjugate IgGMT. *Mol. BioSyst.* **2008**, *4*, 1209–1211.
13. Blackwell, H. E.; Grubbs, R. H. Highly Efficient Synthesis of Covalently Cross-Linked Peptide Helices by Ring-Closing Metathesis. *Angew. Chem., Int. Ed.* **1998**, *37*, 3281–3284.
14. Schafmeister, C. E.; Po, J.; Verdine, G. L. An All-Hydrocarbon Cross-Linking System for Enhancing the Helicity and Metabolic Stability of Peptides. *J. Am. Chem. Soc.* **2000**, *122*, 5891–5892.
15. Croce, T. A.; Hamilton, S. K.; Chen, M. L.; Muchalski, H.; Harth, E. Alternative *O*-Quinodimethane Cross-Linking Precursors for Intramolecular Chain Collapse Nanoparticles. *Macromolecules* **2007**, *40*, 6028–6031.
16. Harth, E.; Van Horn, B.; Lee, V. Y.; Germack, D. S.; Gonzales, C. P.; Miller, R. D.; Hawker, C. J. A Facile Approach to Architecturally Defined Nanoparticles *via* Intramolecular Chain Collapse. *J. Am. Chem. Soc.* **2002**, *124*, 8653–8660.
17. Zhang, L. F.; Chan, J. M.; Gu, F. X.; Rhee, J. W.; Wang, A. Z.; Radovic-Moreno, A. F.; Alexis, F.; Langer, R.; Farokhzad, O. C. Self-Assembled Lipid-Polymer Hybrid Nanoparticles: A Robust Drug Delivery Platform. *ACS Nano* **2008**, *2*, 1696–1702.
18. Elegbede, A. I.; Banerjee, J.; Hanson, A. J.; Tobwala, S.; Ganguli, B.; Wang, R. Y.; Lu, X. N.; Srivastava, D. K.; Mallik, S. Mechanistic Studies of the Triggered Release of Liposomal Contents by Matrix Metalloproteinase-9. *J. Am. Chem. Soc.* **2008**, *130*, 10633–10642.
19. Song, W.; Dong, Z.; Jin, T.; Mantellini, M. G.; Nunez, G.; Nor, J. E. Cancer Gene Therapy with Icaspase-9 Transcriptionally Targeted to Tumor Endothelial Cells. *Cancer Gene Ther.* **2008**, *15*, 667–675.
20. Agarwal, A.; Mallapragada, S. K. Synthetic Sustained Gene Delivery Systems. *Curr. Top. Med. Chem.* **2008**, *8*, 311–330.
21. Carlsson, J.; Drevin, H.; Axen, R. Protein Thiolation and Reversible Protein−Protein Conjugation—*N*-Succinimidyl 3-(2-Pyridyldithio)Propionate, A New Heterobifunctional Reagent. *Biochem. J.* **1978**, *173*, 723–737.